

Article

# Structural Identification of Binary Tetrahydrofuran + O<sub>2</sub> and 3-Hydroxytetrahydrofuran + O<sub>2</sub> Clathrate Hydrates by Rietveld Analysis with Direct Space Method

Yun-Ho Ahn <sup>1</sup>, Byeongwan Lee <sup>2</sup> and Kyuchul Shin <sup>2,\*</sup>

<sup>1</sup> School of Chemical and Biomolecular Engineering, Georgia Institute of Technology, Atlanta, GA 30318, USA; yunho09@gmail.com

<sup>2</sup> Department of Applied Chemistry, School of Applied Chemical Engineering, Kyungpook National University, Daegu 41566, Korea; happyboy0222@naver.com

\* Correspondence: kyuchul.shin@knu.ac.kr; Tel.: +82-53-950-5587

Received: 24 July 2018; Accepted: 14 August 2018; Published: 18 August 2018



**Abstract:** The structural determination of clathrate hydrates, nonstoichiometric crystalline host-guest materials, is challenging because of the dynamical disorder and partial cage occupancies of the guest molecules. The application of direct space methods with Rietveld analysis can determine the powder X-ray diffraction (PXRD) patterns of clathrates. Here, we conducted Rietveld analysis with the direct space method for the structural determination of binary tetrahydrofuran (THF) + O<sub>2</sub> and 3-hydroxytetrahydrofuran (3-OH THF) + O<sub>2</sub> clathrate hydrates in order to identify the hydroxyl substituent effect on interactions between the host framework and the cyclic ether guest molecules. The refined PXRD results reveal that the hydroxyl groups are hydrogen-bonded to host hexagonal rings of water molecules in the 5<sup>12</sup>6<sup>4</sup> cage, while any evidences of hydrogen bonding between THF guests and the host framework were not observed from PXRD at 100 K. This guest-host hydrogen bonding is thought to induce slightly larger 5<sup>12</sup> cages in the 3-OH THF hydrate than those in the THF hydrate. Consequently, the disorder dynamics of the secondary guest molecules also can be affected by the hydrogen bonding of larger guest molecules. The structural information of binary clathrate hydrates reported here can improve the understanding of the host-guest interactions occurring in clathrate hydrates and the specialized methodologies for crystal structure determination of clathrate hydrates.

**Keywords:** clathrate hydrate; powder X-ray diffraction; Rietveld refinement

## 1. Introduction

Clathrate hydrates are nonstoichiometric crystalline host-guest compounds stabilized by van der Waals interactions between hydrogen-bonded water cages and hydrophobic guest molecules [1,2]. Because they have high capacities for gas storage reaching 170 *v/v*, clathrate hydrates are potentially applicable in the areas of gas storage, separation, transportation, and carbon sequestration [3–6]. In nature, natural gas clathrate hydrates are abundant in permafrost or subsea sediment regions; hence, clathrate hydrates of natural gases are also considered as potential energy resources [7–11]. For application as gas storage materials or as natural gas sources, the understanding of the physicochemical properties of clathrate hydrates, including thermodynamic stability, guest distributions and occupancies, and formation kinetics, is essential. The structural characterization of such materials regarding host-guest interactions is thus a prerequisite for an improved understanding of the inherent nature of clathrate hydrates. However, structural determination of clathrate hydrates is challenging because of dynamical disorder and partial cage occupancies of the guest molecules.

In particular, X-ray diffraction analysis for the structural characterization of powdered clathrate hydrate samples is often difficult because clathrate hydrates contain many hydrogen atoms. The contributions of hydrogen atoms to the diffraction patterns are significant, but the atomic scattering factor of hydrogen is too small to use for the analysis of low-resolution powder diffraction patterns.

Recently, Takeya et al. reported that the application of direct space methods with Rietveld analysis can solve powder X-ray diffraction (PXRD) patterns of these clathrate hydrate materials [12]. They suggested that the position of rigid body guest molecules in the cages of the fixed host framework can be determined by a Monte-Carlo approach minimizing reliability factors of refined patterns and also demonstrated that the dynamical disorder of guest molecules in the cages of structure I (sI; cubic  $Pm-3n$ ), structure II (sII; cubic  $Fd-3m$ ), and structure H (sH; hexagonal  $P6/mmm$ ) clathrate hydrates can be refined by the direct-space technique. To overcome the limitation of the small scattering amplitude of hydrogen atoms, they used virtual chemical species with sums of atomic scattering factors instead of refining the hydrogen positions. Shin et al. demonstrated that the hydrogen atom positions of host water molecules can be refined with some distance constraints between oxygen and hydrogen atoms of water molecules when synchrotron high-resolution powder diffraction data were used [13]. Therefore, structural determination of clathrate hydrates including hydrogen atom positions can be achieved by Rietveld refinement analysis with the direct space method of high-resolution PXRD patterns.

Three widely known crystal structures of clathrate hydrates exist [1,2]. The sI hydrate, whose lattice parameter is  $\sim 12 \text{ \AA}$ , contains six tetrakaidecahedrons ( $5^{12}6^2$ ) and two pentagonal dodecahedrons ( $5^{12}$ ) cages in the unit cell comprising 46  $\text{H}_2\text{O}$  molecules. The sII hydrate, whose lattice parameter is  $\sim 17.3 \text{ \AA}$ , contains eight hexakaidecahedrons ( $5^{12}6^4$ ) and sixteen  $5^{12}$  cages in the unit cell comprising 136  $\text{H}_2\text{O}$  molecules. The sH hydrate, with the lattice parameters  $a \sim 12.2 \text{ \AA}$  and  $c \sim 10.1 \text{ \AA}$ , contains one icosahedron ( $5^{12}6^8$ ), two irregular dodecahedrons ( $4^35^66^3$ ), and three  $5^{12}$  cages in the unit cell comprising 34  $\text{H}_2\text{O}$  molecules. Some decades ago, canonical clathrate hydrates were thought to be stabilized by van der Waals interactions only, without any directional guest-host interactions [1,14]. However, recent studies have revealed that hydrogen bonding or halogen bonding between the host and guest molecules occasionally occurs in clathrate hydrate phases [14–20].

Here, we conducted Rietveld analysis with the direct space method for the structural determination of binary tetrahydrofuran (THF) +  $\text{O}_2$  and 3-hydroxytetrahydrofuran (3-OH THF) +  $\text{O}_2$  clathrate hydrates in order to identify the hydroxyl substituent effect on interactions between the host framework and cyclic ether guest molecules. THF is a widely known hydrate-forming cyclic ether that occupies the  $5^{12}6^4$  cages of sII hydrate [1,2,21–23]. On the other hand, 3-OH THF, a hydroxyl group substituted THF, cannot form sII hydrate alone but can form a sII hydrate with secondary gaseous guest molecules such as  $\text{O}_2$ ,  $\text{N}_2$ , or  $\text{CH}_4$  [24]. Because of the inhibition effect of the hydroxyl group, binary (3-OH THF + gaseous guest) hydrates are thermodynamically less stable than binary THF hydrates. In this work, high-resolution PXRD patterns of THF +  $\text{O}_2$  and 3-OH THF +  $\text{O}_2$  binary hydrates were obtained from a synchrotron beam line and refined by the direct space method and Rietveld method in order to investigate the effect of hydroxyl groups on enclathrated cyclic ether guest molecules.

## 2. Experimental Section

THF and 3-OH THF were supplied by Sigma-Aldrich Inc. (St. Louis, MO, USA) and used without further purification.  $\text{O}_2$  gas of 99.95 mol % purity was purchased from Special Gas (Daejeon, Korea).

A well-mixed solution of THF/ $\text{H}_2\text{O}$  or 3-OH THF/ $\text{H}_2\text{O}$  at the mole ratio of 1:17 was prepared. A high-pressure reactor with an internal volume of 50 mL was loaded with 10 g of each solution and then placed in a refrigerated ethanol circulator (RW-2025G, Jeio Tech Co., Ltd., Daejeon, Korea) and pressurized by  $\text{O}_2$  up to 12 MPa at 293 K. The fluids inside the reactor were mechanically stirred throughout hydrate formation. After the system reached the steady state, the reactor was slowly cooled to 253 K and maintained at that temperature for three days. The synthesized hydrate samples were collected and finely ground at liquid nitrogen temperature. The powdered samples were kept in a liquid nitrogen storage dewar until diffraction pattern measurement.

The PXRD patterns were obtained using the supramolecular crystallography beamline (2D) at the Pohang Accelerator Laboratory (PAL) in Korea. An ADSC Quantum 210 CCD detector (210 mm × 210 mm) with synchrotron radiation ( $\lambda = 0.9000 \text{ \AA}$ ) was used. A pre-cooled polyimide tube (purchased from Cole-Parmer, Vernon Hills, IL, USA); inner diameter: 0.025 in; outer diameter: 0.269 in) was filled with the powdered hydrate sample and loaded into the diffractometer. The sample-detector distance was 63 mm. Two-dimensional patterns of 4096 pixels by 4096 pixels were recorded with an exposure time of 5 s at 100 K and then were converted into one-dimensional diffraction patterns of  $2\theta$  range from 0 to  $66.9932^\circ$ . As the intensities near the starting and endpoints of the patterns diverged, the  $2\theta$  regions from 0 to 4 and from 66 to endpoint were excluded. The obtained patterns were refined by Rietveld analysis with the direct space method [12]. The guest molecules of THF, 3-OH THF, and  $\text{O}_2$  were assumed as rigid bodies, and their positions were determined by the direct space method using the program FOX [25,26]. With these initial guest coordinates, the patterns were refined by the Rietveld method with the FULLPROF program [27]. During the refinements, soft distance constraints for the host water molecules (O-H covalent bond length: 0.98 Å; and O-H hydrogen bond length: 1.74 Å) were applied. The isotropic atomic displacement parameters for hydrogen atoms can be experientially constrained to be some factor times the values for the atoms to which the hydrogens are bonded [28]. In this work, the isotropic temperature factor ( $B$  value, defined as  $B = 8\pi^2\langle u^2 \rangle$  where  $\langle u^2 \rangle$  is the mean square isotropic displacement) of a hydrogen atom of  $\text{H}_2\text{O}$ , THF, or 3-OH THF was assumed to be 1.5 times the  $B$  value factor of the atom to which the hydrogen was bonded [29]. The  $B$  values for the carbon and oxygen atoms of THF or 3-OH THF were defined as identical.

### 3. Results and Discussion

The atomic coordinates, isotropic temperature factors, and site occupancies of THF +  $\text{O}_2$  and 3-OH THF +  $\text{O}_2$  hydrates, which were determined by Rietveld analysis with the direct space method, are presented in Tables 1 and 2.

**Table 1.** Atomic coordinates and isotropic temperature factors for binary tetrahydrofuran (THF) +  $\text{O}_2$  hydrate at 100 K.  $\text{H}_{ea}$ : hydrogen covalently connected with  $\text{O}_e$  and hydrogen bonded with  $\text{O}_a$  ( $\text{O}_e\text{-H}_{ea}\text{-O}_a$ ).  $\text{H}_{gg}(\text{p})$ : hydrogen in pentagonal ring; and  $\text{H}_{gg}(\text{h})$ : in hexagonal ring. Site: multiplicity and Wyckoff letter.

Atom	$x$	$y$	$z$	$B$ (Å <sup>2</sup> )	$g$	Site
$\text{O}_a$	0.125	0.125	0.125	1.84 (10)	1	8 $a$
$\text{O}_e$	0.2166 (1)	0.2166	0.2166	1.56 (6)	1	32 $e$
$\text{O}_g$	0.1822 (1)	0.1822	0.3706 (1)	1.80 (3)	1	96 $g$
$\text{H}_{ea}$	0.1842 (2)	0.1842	0.1842	2.34	0.5	32 $e$
$\text{H}_{ae}$	0.1581 (2)	0.1581	0.1581	2.76	0.5	32 $e$
$\text{H}_{eg}$	0.2106 (10)	0.2106	0.2731 (6)	2.34	0.5	96 $g$
$\text{H}_{ge}$	0.1827 (10)	0.1827	0.3110 (5)	2.70	0.5	96 $g$
$\text{H}_{gg}(\text{p})$	0.1414 (3)	0.1414	0.3640 (19)	2.70	0.5	96 $g$
$\text{H}_{gg}(\text{h})$	0.2373 (7)	0.1807 (8)	0.3912 (11)	2.70	0.5	192 $i$
$\text{C}_L1$	0.9314	0.9142	0.3679	3.43 (29)	0.0415 (2)	192 $i$
$\text{O}_L2$	0.9143	0.8484	0.3197	3.43	0.0415	192 $i$
$\text{C}_L3$	0.8364	0.8600	0.2924	3.43	0.0415	192 $i$
$\text{C}_L4$	0.7909	0.8937	0.3624	3.43	0.0415	192 $i$
$\text{C}_L5$	0.8557	0.9311	0.4138	3.43	0.0415	192 $i$
$\text{H}_L6$	0.9811	0.8990	0.4045	5.14	0.0415	192 $i$
$\text{H}_L7$	0.9474	0.9644	0.3312	5.14	0.0415	192 $i$
$\text{H}_L8$	0.8365	0.9012	0.2433	5.14	0.0415	192 $i$
$\text{H}_L9$	0.8146	0.8039	0.2718	5.14	0.0415	192 $i$
$\text{H}_L10$	0.7471	0.9359	0.3438	5.14	0.0415	192 $i$
$\text{H}_L11$	0.7609	0.8473	0.3941	5.14	0.0415	192 $i$
$\text{H}_L12$	0.8576	0.9038	0.4712	5.14	0.0415	192 $i$
$\text{H}_L13$	0.8469	0.9936	0.4223	5.14	0.0415	192 $i$
$\text{O}_S1$	0.2317	0.2285	0.9789	5.31 (19)	0.0808 (4)	192 $i$
$\text{O}_S2$	0.2775	0.2695	1.0131	5.31	0.0808	192 $i$

**Table 2.** Atomic coordinates and isotropic temperature factors for 3-hydroxytetrahydrofuran (3-OH THF) + O<sub>2</sub> hydrate at 100 K.

Atom	<i>x</i>	<i>y</i>	<i>z</i>	<i>B</i> (Å <sup>2</sup> )	<i>g</i>	Site
O <sub>a</sub>	0.125	0.125	0.125	1.42 (9)	1	8 <i>a</i>
O <sub>e</sub>	0.2166 (1)	0.2166	0.2166	1.55 (6)	1	32 <i>e</i>
O <sub>g</sub>	0.1824 (1)	0.1824	0.3708 (1)	1.90 (3)	1	96 <i>g</i>
H <sub>ea</sub>	0.1842 (2)	0.1842	0.1842	2.32	0.5	32 <i>e</i>
H <sub>ae</sub>	0.1578 (2)	0.1578	0.1578	2.13	0.5	32 <i>e</i>
H <sub>eg</sub>	0.2156 (9)	0.2156	0.2752 (5)	2.32	0.5	96 <i>g</i>
H <sub>ge</sub>	0.1857 (11)	0.1857	0.3127 (6)	2.85	0.5	96 <i>g</i>
H <sub>gg(p)</sub>	0.1416 (3)	0.1416	0.3835 (15)	2.85	0.5	96 <i>g</i>
H <sub>gg(h)</sub>	0.2372 (7)	0.1782 (9)	0.3878 (12)	2.85	0.5	192 <i>i</i>
C <sub>L1</sub>	0.6740	0.1037	0.1417	1.89 (34)	0.0387 (2)	192 <i>i</i>
O <sub>L2</sub>	0.6493	0.0585	0.0732	1.89	0.0387	192 <i>i</i>
C <sub>L3</sub>	0.5662	0.0766	0.0571	1.89	0.0387	192 <i>i</i>
C <sub>L4</sub>	0.5426	0.1418	0.1146	1.89	0.0387	192 <i>i</i>
C <sub>L5</sub>	0.5986	0.1280	0.1841	1.89	0.0387	192 <i>i</i>
H <sub>L6</sub>	0.7121	0.0671	0.1774	2.83	0.0387	192 <i>i</i>
H <sub>L7</sub>	0.7047	0.1574	0.1252	2.83	0.0387	192 <i>i</i>
H <sub>L8</sub>	0.5601	0.0947	−0.0039	2.83	0.0387	192 <i>i</i>
H <sub>L9</sub>	0.5315	0.0237	0.0668	2.83	0.0387	192 <i>i</i>
H <sub>L10</sub>	0.5564	0.1996	0.0909	2.83	0.0387	192 <i>i</i>
H <sub>L11</sub>	0.4809	0.1392	0.1307	2.83	0.0387	192 <i>i</i>
H <sub>L12</sub>	0.5771	0.0795	0.2203	2.83	0.0387	192 <i>i</i>
O <sub>L13</sub>	0.6164	0.1972	0.2297	1.89	0.0387	192 <i>i</i>
H <sub>L14</sub>	0.5686	0.2118	0.2593	2.83	0.0387	192 <i>i</i>
O <sub>S1</sub>	0.2829	0.2292	0.9757	4.27 (25)	0.0785 (5)	192 <i>i</i>
O <sub>S2</sub>	0.2440	0.2626	1.0236	4.27	0.0785	192 <i>i</i>

THF is a widely known sII hydrate former. As expected, the pattern of THF + O<sub>2</sub> hydrate sample in Figure 1a shows the cubic *Fd-3m* structure with a lattice parameter of  $a = 17.1143(5)$  Å. The calculated density is 1.166 g/cm<sup>3</sup>. As reported previously [24], the pattern of the 3-OH THF + O<sub>2</sub> hydrate sample also shows the cubic *Fd-3m* structure with a lattice parameter of  $a = 17.1268(5)$  Å, with a tiny amount of hexagonal ice impurities (Figure 1b). The calculated density of the hydrate phase is 1.186 g/cm<sup>3</sup>. The refined cage occupancy values for THF and 3-OH THF in the 5<sup>12</sup>6<sup>4</sup> cages are 1.00 (1) and 0.93 (1), respectively (Tables 1 and 2). The slightly smaller value of the latter system may arise from the nature of the 3-OH THF molecule, which cannot form the sII hydrate on its own. Although 3-OH THF is a larger guest molecule than THF (Figure 2), the estimated average radii (average distances between the cage centers and each oxygen atom) of the 5<sup>12</sup>6<sup>4</sup> cages are almost equal at 4.629 Å and 4.630 Å for the THF and 3-OH THF hydrates, respectively. Here, we assumed that the 5<sup>12</sup>6<sup>4</sup> cages are occupied by only large hydrocarbon molecules in both the THF and 3-OH THF hydrates in this work. Although a possibility of O<sub>2</sub> occupancy in the 5<sup>12</sup>6<sup>4</sup> cages of the 3-OH THF hydrate exists, the number of small guest molecules occupying the large cages is usually ignorable when a stoichiometric amount of large guest molecules for sII hydrate is used.

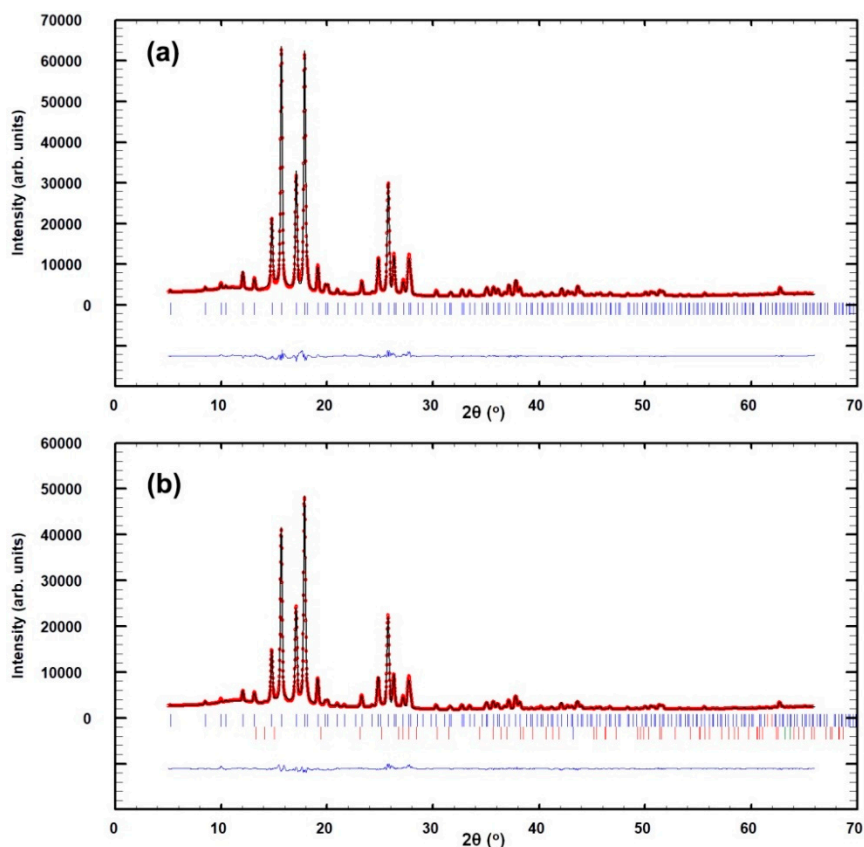


**Figure 1.** (a) Rietveld refinement of the THF + O<sub>2</sub> hydrate pattern. Space group: *Fd-3m*; Lattice parameter:  $a = 17.1143$  (5) Å; Reliability factors:  $\chi^2 = 5.68$ ; and  $R_{wp} = 8.55\%$  (background subtracted); (b) Rietveld refinement of the 3-OH THF + O<sub>2</sub> hydrate pattern (tick marks: first row for sII hydrate, second row for ice I<sub>h</sub>). Space group: *Fd-3m*; Lattice parameter:  $a = 17.1268$  (5) Å; Reliability factors:  $\chi^2 = 3.65$ ; and  $R_{wp} = 8.38\%$  (background subtracted).

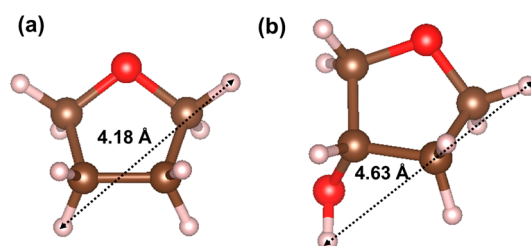


**Figure 2.** Molecular shapes and the longest end-to-end distances of (a) THF and (b) 3-OH THF.

The hydroxyl group capable of hydrogen bonding is usually allowed to approach the host water molecules more closely than other hydrophobic groups in the guest molecules [15,20,30,31]; this may explain the 3-OH THF formation of the sII hydrate, while 2-methyl THF, which is similar in size, forms the sH hydrate with the assistance of CH<sub>4</sub> or Xe gases [32].

Figures 3 and 4 show the crystal structures and guest positions of the THF + O<sub>2</sub> and 3-OH THF + O<sub>2</sub> hydrates as obtained by Rietveld refinement.

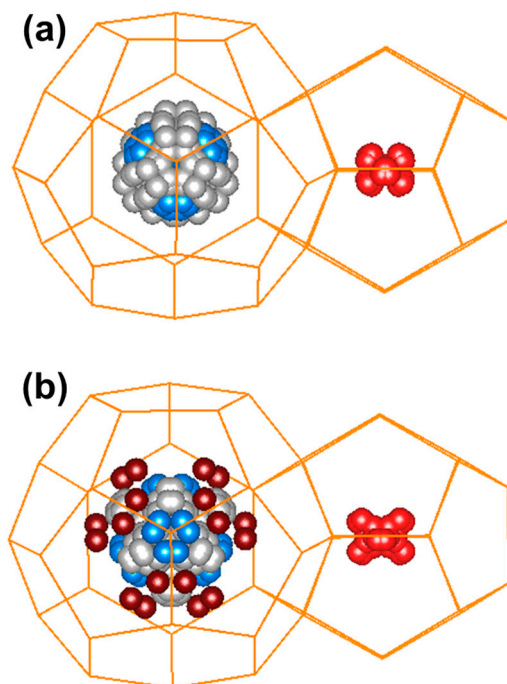


**Figure 3.** Guest distributions with full symmetry in  $5^{12}6^4$  and  $5^{12}$  cages. (a) THF + O<sub>2</sub> and (b) 3-OH THF + O<sub>2</sub> hydrates. (Red: oxygen of O<sub>2</sub> molecule; Gray: carbon; blue: oxygen in cyclic rings; brown: oxygen of hydroxyl group. Hydrogen atoms are omitted.).

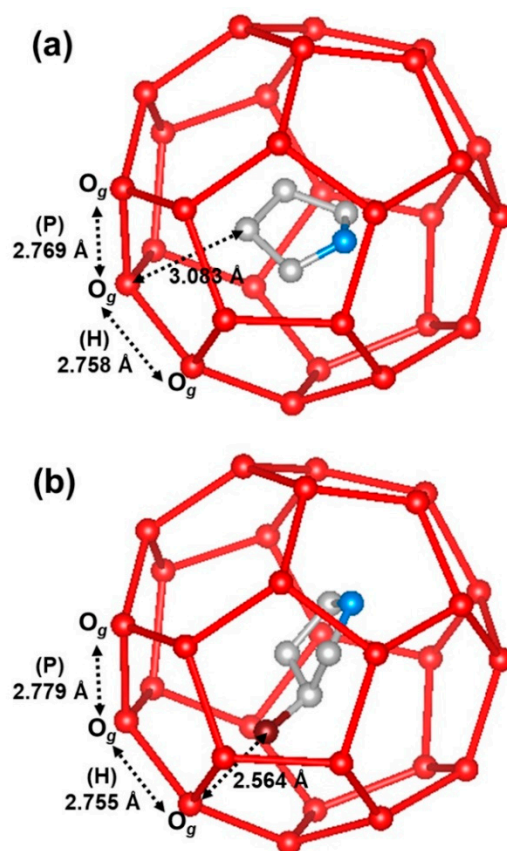


**Figure 4.** Guest molecules in the  $5^{12}6^4$  cages of (a) THF + O<sub>2</sub> and (b) 3-OH THF + O<sub>2</sub> hydrates.

As shown in Figure 3a, THF molecules are spherically distributed in the  $5^{12}6^4$  cages. The shortest distance between a host oxygen atom and guest carbon or oxygen atom is calculated as 3.083 Å (Figure 4a). On the other hand, Figure 3b shows that the hydroxyl groups of 3-OH THF are oriented toward the hexagonal faces of the  $5^{12}6^4$  cages. The shortest host-guest distance between oxygen atoms is calculated as 2.564 Å (Figure 4b); the PXRD analysis thus reveals that the hydroxyl functional group of 3-OH THF is hydrogen-bonded to the host water molecules. As H<sub>2</sub>O molecules in the sII hydrates are tetrahedrally connected to each other, the hexagonal rings in the  $5^{12}6^4$  cages are relatively weakly hydrogen-bonded in the host framework (the O-O-O angles are  $\sim 120^\circ$ , whereas those in pentagonal rings are  $\sim 108^\circ$ ). Therefore, the guest-host hydrogen bonding in the  $5^{12}6^4$  cage often occurs at the hexagonal rings, as shown in Figures 3b and 4b [18–20].

The distances between host oxygen atoms can be affected by the guest-host hydrogen bonding. In the THF + O<sub>2</sub> hydrate, the O<sub>g</sub>-O<sub>g</sub> distances in the hexagonal and pentagonal faces are calculated as 2.758 Å and 2.769 Å, respectively (Figure 4). On the other hand, those distances for the 3-OH THF + O<sub>2</sub> hydrate are 2.755 Å and 2.779 Å in the hexagonal and pentagonal faces, respectively. The slightly larger difference in the O<sub>g</sub>-O<sub>g</sub> distance between the hexagonal and pentagonal faces of the 3-OH THF + O<sub>2</sub> hydrate suggests a slightly distorted framework in the 3-OH THF + O<sub>2</sub> hydrate, caused by the guest-host hydrogen bonding. The host O-O distances are listed in Table 3.

**Table 3.** Distances of host O-O atoms in the THF + O<sub>2</sub> and 3-OH THF + O<sub>2</sub> hydrates.

Hydrates	O <sub>a</sub> -O <sub>e</sub> (Å)	O <sub>e</sub> -O <sub>g</sub> (Å)	O <sub>g</sub> -O <sub>g</sub> (p) <sup>1</sup> (Å)	O <sub>g</sub> -O <sub>g</sub> (h) <sup>2</sup> (Å)
THF + O <sub>2</sub>	2.714 (2)	2.765 (2)	2.769 (2)	2.758 (3)
3-OH THF + O <sub>2</sub>	2.716 (2)	2.768 (3)	2.779 (2)	2.755 (3)

<sup>1</sup> in the pentagonal ring; <sup>2</sup> in the hexagonal ring.

The average radii of the small  $5^{12}$  cages for both hydrates are also estimated; the values are 3.858 Å for the THF hydrate and 3.862 Å for the 3-OH THF hydrate. The  $5^{12}$  cages in the latter are slightly larger than those in the former. This can be a result of framework distortion induced by the significant guest-host hydrogen bonding occurring in the large  $5^{12}6^4$  cage of 3-OH THF hydrate. The off-centered distances of the O<sub>2</sub> guest molecules from the centers of the  $5^{12}$  cages are calculated at 0.11 Å and 0.24 Å for the THF and 3-OH THF hydrates, respectively. The estimated  $5^{12}$  cage radii and the off-centered distances support that the position of the O<sub>2</sub> guest molecule in the 3-OH THF hydrate fluctuates more as shown in Figure 3, representing the disorder dynamics of the guest molecules. However, as the mean square isotropic displacement ( $\langle u^2 \rangle$ ) of guest O atoms in THF hydrate, meaning thermal vibration amplitude of O atom, is slightly larger (0.067(2) Å<sup>2</sup> for the THF hydrate and 0.054 (3) Å<sup>2</sup> for the 3-OH THF hydrate) than the value in the 3-OH THF hydrate, it is difficult to conclude that the O<sub>2</sub> guest molecules captured in the 3-OH THF hydrate occupy more space than those in the THF hydrate.

#### 4. Conclusions

In this work, the PXRD patterns of the two binary clathrate hydrates of THF + O<sub>2</sub> and 3-OH THF + O<sub>2</sub> were analyzed by Rietveld refinement with the direct space method. The hydroxyl group of 3-OH THF was hydrogen-bonded to the host water molecules in the hexagonal rings of the  $5^{12}6^4$  cages. This guest-host hydrogen bonding slightly distorted the framework and is thought to induce larger  $5^{12}$  cage in the 3-OH THF hydrate. Consequentially, the disorder dynamics of the secondary small guest molecules also can be affected by hydrogen bonding between large guest molecules and the host framework. The findings presented in this work can provide a better understanding of host-guest interactions occurring in clathrate hydrates and the specialized methodologies for the crystal structure determination of clathrate hydrates.

**Author Contributions:** Conceptualization, K.S. and Y.-H.A.; Methodology, Y.-H.A. and K.S.; Software, K.S.; Validation, K.S., Y.-H.A. and B.L.; Formal Analysis, K.S. and B.L.; Investigation, Y.-H.A.; Resources, K.S.; Data Curation, K.S., Y.-H.A. and B.L.; Writing-Original Draft Preparation, K.S.; Writing-Review & Editing, K.S., Y.-H.A. and B.L.; Visualization, K.S.; Supervision, K.S.; Project Administration, K.S.; Funding Acquisition, K.S.

**Funding:** This work was supported by the National Research Foundation of Korea (NRF) grant (NRF-2018R1D1A1B07040575) funded by the Ministry of Education (MOE) and the Korea Institute of Energy Technology Evaluation and Planning (KETEP) grant (No. 20141510300310) funded by the Ministry of Trade, Industry & Energy (MOTIE).

**Acknowledgments:** PXRD experiments were performed at the beamline 2D of the Pohang Accelerator Laboratory (PAL).

**Conflicts of Interest:** The authors declare no conflicts of interest.

## References

1. Jeffrey, G.A. *Inclusion Compounds*; Atwood, J.L., Davies, J.E.D., MacNicol, D.D., Eds.; Academic Press: London, UK, 1984; Volume 1, pp. 135–190.
2. Sloan, E.D.; Koh, C.A. *Clathrate Hydrates of Natural Gases*, 3rd ed.; CRC Press, Taylor & Francis Group: Boca Raton, FL, USA, 2008.
3. Wang, W.; Bray, C.L.; Adams, D.J.; Cooper, A.I. Methane Storage in Dry Water Gas Hydrates. *J. Am. Chem. Soc.* **2008**, *130*, 11608–11609. [[CrossRef](#)] [[PubMed](#)]
4. Kang, S.P.; Lee, H. Recovery of CO<sub>2</sub> from Flue Gas Using Gas Hydrate: Thermodynamic Verification through Phase Equilibrium Measurements. *Environ. Sci. Technol.* **2000**, *34*, 4397–4400. [[CrossRef](#)]
5. Stern, L.A.; Circone, S.; Kirby, S.H.; Durham, W.B. Temperature, Pressure, and Compositional Effects on Anomalous or “Self” Preservation of Gas Hydrates. *Can. J. Phys.* **2003**, *81*, 271–283. [[CrossRef](#)]
6. Babu, P.; Kumar, R.; Linga, P. Pre-Combustion Capture of Carbon Dioxide in a Fixed Bed Reactor Using the Clathrate Hydrate Process. *Energy* **2013**, *50*, 364–373. [[CrossRef](#)]
7. Koh, C.A.; Sum, A.K.; Sloan, E.D. State of the Art: Natural Gas Hydrates as a Natural Resource. *J. Nat. Gas Sci. Eng.* **2012**, *8*, 132–138. [[CrossRef](#)]
8. Ohgaki, K.; Takano, K.; Sangawa, H.; Matsubara, T.; Nakano, S. Methane Exploitation by Carbon Dioxide from Gas Hydrates Phase Equilibria for CO<sub>2</sub>-CH<sub>4</sub> Mixed Hydrate System. *J. Chem. Eng. Jpn.* **1996**, *29*, 478–483. [[CrossRef](#)]
9. Lee, H.; Seo, Y.; Seo, Y.T.; Moudrakovski, I.L.; Ripmeester, J.A. Recovering Methane from Solid Methane Hydrate with Carbon Dioxide. *Angew. Chem. Int. Ed.* **2003**, *42*, 5048–5051. [[CrossRef](#)] [[PubMed](#)]
10. Bai, D.; Zhang, X.; Chen, G.; Wang, W. Replacement Mechanism of Methane Hydrate with Carbon Dioxide from Microsecond Molecular Dynamic Simulations. *Energy Environ. Sci.* **2012**, *5*, 7033–7041. [[CrossRef](#)]
11. Chong, Z.R.; Yang, S.H.B.; Babu, P.; Linga, P.; Li, X.-S. Review of Natural Gas Hydrates as an Energy Resource: Prospects and Challenges. *Appl. Energy* **2016**, *162*, 1633–1652. [[CrossRef](#)]
12. Takeya, S.; Udachin, K.A.; Moudrakovski, I.L.; Susilo, R.; Ripmeester, J.A. Direct Space Methods for Powder X-ray Diffraction for Guest-Host Materials: Applications to Cage Occupancies and Guest Distributions in Clathrate Hydrates. *J. Am. Chem. Soc.* **2010**, *132*, 524–531. [[CrossRef](#)] [[PubMed](#)]
13. Shin, K.; Cha, M.; Lee, W.; Seo, Y.; Lee, H. Abnormal Proton positioning of Water Framework in the Presence of Paramagnetic Guest within Ion-Doped Clathrate Hydrate Host. *J. Phys. Chem. C* **2014**, *118*, 15193–15199. [[CrossRef](#)]
14. Susilo, R.; Alavi, S.; Moudrakovski, I.L.; Englezos, P.; Ripmeester, J.A. Guest-Host Hydrogen Bonding in Structure H Clathrate Hydrates. *ChemPhysChem* **2009**, *10*, 824–829. [[CrossRef](#)] [[PubMed](#)]
15. Alavi, S.; Udachin, K.; Ripmeester, J.A. Effect of Guest-Host Hydrogen Bonding on the Structures and Properties of Clathrate Hydrates. *Chem. Eur. J.* **2010**, *16*, 1017–1025. [[CrossRef](#)] [[PubMed](#)]
16. Udachin, K.A.; Alavi, S.; Ripmeester, J.A. Water-Halogen Interactions in Chlorine and Bromine Clathrate Hydrates: An Example of Multidirectional Halogen Bonding. *J. Phys. Chem. C* **2013**, *117*, 14176–14182. [[CrossRef](#)]
17. Alavi, S.; Takeya, S.; Ohmura, R.; Woo, T.K.; Ripmeester, J.A. Hydrogen-bonding alcohol-water interactions in binary ethanol, 1-propanol, and 2-propanol + methane structure II clathrate hydrates. *J. Chem. Phys.* **2010**, *133*, 074505. [[CrossRef](#)] [[PubMed](#)]

18. Udachin, K.; Alavi, S.; Ripmeester, J.A. Communication: Single Crystal X-ray Diffraction Observation of Hydrogen Bonding between 1-Propanol and Water in a Structure Ii Clathrate Hydrate. *J. Chem. Phys.* **2011**, *134*, 121104. [[CrossRef](#)] [[PubMed](#)]
19. Shin, K.; Kumar, R.; Udachin, K.A.; Alavi, S.; Ripmeester, J.A. Ammonia Clathrate Hydrates as New Solid Phases for Titan, Enceladus, and other Planetary Systems. *Proc. Natl. Acad. Sci. USA* **2012**, *109*, 14785–14790. [[CrossRef](#)] [[PubMed](#)]
20. Shin, K.; Udachin, K.A.; Moudrakovski, I.L.; Leek, D.M.; Alavi, S.; Ratcliffe, C.I.; Ripmeester, J.A. Methanol Incorporation in Clathrate Hydrates and the Implications for Oil and Gas Pipeline Flow Assurance and Icy Planetary Bodies. *Proc. Natl. Acad. Sci. USA* **2013**, *110*, 8437–8442. [[CrossRef](#)] [[PubMed](#)]
21. Jones, C.Y.; Marshall, S.L.; Chakoumakos, B.C.; Rawn, C.J.; Ishii, Y. Structure and Thermal Expansivity of Tetrahydrofuran Deuterate Determined by Neutron Powder Diffraction. *J. Phys. Chem. B* **2003**, *107*, 6026–6031. [[CrossRef](#)]
22. Lee, H.; Lee, J.-W.; Kim, D.Y.; Park, J.; Seo, Y.-T.; Zeng, H.; Moudrakovski, I.L.; Ratcliffe, C.I.; Ripmeester, J.A. Tuning Clathrate Hydrates for Hydrogen Storage. *Nature* **2005**, *434*, 743–746. [[CrossRef](#)] [[PubMed](#)]
23. Florusse, L.J.; Peters, C.J.; Schoonman, J.; Hester, K.C.; Koh, C.A.; Dec, S.F.; Marsh, K.N.; Sloan, E.D. Stable Low-Pressure Hydrogen Clusters Stored in a Binary Clathrate Hydrate. *Science* **2004**, *306*, 469–471. [[CrossRef](#)] [[PubMed](#)]
24. Ahn, Y.-H.; Kang, H.; Koh, D.-Y.; Park, Y.; Lee, H. Gas hydrate Inhibition by 3-Hydroxytetrahydrofuran: Spectroscopic Identifications and Hydrate Phase Equilibria. *Fluid Phase Equilib.* **2016**, *413*, 65–70. [[CrossRef](#)]
25. Favre-Nicolin, F.; Cerny, R. ‘Free objects for crystallography’: A Modular Approach to Ab Initio Structure Determination from Powder Diffraction. *J. Appl. Crystallogr.* **2002**, *35*, 734–743. [[CrossRef](#)]
26. Cerny, R.; Favre-Nicolin, F. Direct Space Methods of Structure Determination from Powder Diffraction: Principles, Guidelines and Perspectives. *Z. Kristallogr.* **2007**, *222*, 105–113.
27. Rodriguez-Carvajal, J. Recent Advances in Magnetic Structure Determination by Neutron Powder Diffraction. *Phys. B* **1993**, *192*, 55–69. [[CrossRef](#)]
28. Massa, W. *Crystal Structure Determination*, 2nd ed.; Springer: New York, NY, USA, 2004.
29. Kirchner, M.T.; Boese, R.; Billups, W.E.; Norman, L.R. Gas Hydrate Single-Crystal Structure Analyses. *J. Am. Chem. Soc.* **2004**, *126*, 9407–9412. [[CrossRef](#)] [[PubMed](#)]
30. Alavi, S.; Susilo, R.; Ripmeester, J.A. Linking Microscopic Guest Properties to Macroscopic Observables in Clathrate Hydrates: Guest-Host Hydrogen Bonding. *J. Chem. Phys.* **2009**, *130*, 174501. [[CrossRef](#)] [[PubMed](#)]
31. Alavi, S.; Shin, K.; Ripmeester, J.A. Molecular Dynamics Simulations of Hydrogen Bonding in Clathrate Hydrates with Ammonia and Methanol Guest Molecules. *J. Chem. Eng. Data* **2015**, *60*, 389–397. [[CrossRef](#)]
32. Lee, J.-W.; Lu, H.; Moudrakovski, I.L.; Ratcliffe, C.I.; Ripmeester, J.A. Thermodynamic and molecular-scale analysis of new systems of water-soluble hydrate formers+ CH<sub>4</sub>. *J. Phys. Chem. B* **2010**, *114*, 13393–13398. [[CrossRef](#)] [[PubMed](#)]

